Engineered Science
DOI: https://dx.doi.org/10.30919/es1307

Oscillating Electromagnetic Field Effect on Nusselt Number and Pressure Drop of Ferrofluid in the Fluted Tubes

Ponthep Vengsungnle,[1] Jarinee Jongpleumpiti,[1] Nittaya Naphon,[2] Sahassawas Poojeera,[3] Apichat Srichat,[4] Smith Eiamsa-ard[5] and Paisarn Naphon[6,*]

Abstract

The heat transfer and friction factor of ferrofluid passing a helically fluted tube with a constant and oscillating electromagnetic field were experimentally investigated. The sixteen electromagnet units, the monitor system, and the Programmable Logic Controller (PLC) system comprise the electromagnetic field (EF) system. The use of Ferrosoferric oxide (Fe_3O_4) nanoparticles in this work is based on the excellent response to the electromagnetic field. An experiment with the corrugated tube had inside diameter, outside diameters, and length values of 1.02 cm, 1.27 cm, and 200 cm, respectively. The effect of the electromagnetic rotating direction, flux, frequency, and frequency on the heat removal capability and flow resistance have been considered. It can be seen that increasing the electromagnetic flux and frequency may significantly increase the heat-removal capacity. The average Nusselt number rises by 2.54 %, 5.32 %, and 12.32 % for the electromagnetic field 0.5 μT, 1.4 μT, and 20 μT, respectively, compared with the absent electromagnetic field. Moreover, the Brownian motion of particles greatly influences the electromagnetic rotation direction, power, and frequency, leading to increased heat transfer. The friction factor is also further increased by the disruption of electromagnetic flow. Despite this, the impact is not as significant as the augmentation of heat transport.

Keywords: Electromagnet field; Oscillation; Ferrofluid; Fluted tube.
Received: 16 July 2024; Revised: 23 August 2024; Accepted: 04 September 2024.
Article type: Research article.

1. Introduction

Heat dissipation must be better than heat created to sustain operation and guarantee the dependability of the electronic devices. The heat transfer augmentation method was divided into passive and active categories. Active methods require power sources, including magnetic fields or pulsing fluid flow, whereas passive methods concentrate on surface additions or configurations to enhance their characteristics. Several studies looked at ways to improve heat transmission. Li *et al*.[1] conducted studies to look into the transport characteristics of magnetic fluids. It has been demonstrated that as magnetic field strengths rise, so does the thermal conductivity of magnetic nanofluids. Li and Xuan studied the heat capability around a thin wire in the magnetic field.[2] The heat transfer enhancement of magnetic liquid with the magnetic field was examined by Lajvardi *et al*.[3] Using a binary ferrofluid in thermal devices with a magnetic drive was studied.[4] Experiments were undertaken by Darzi *et al*.[5] to consider the turbulent flow behavior in helically corrugated pipes. The heat removal efficiency of these devices was greatly affected by the coolant's altered thermal conductivity.[6-8] Researchers investigated the applicability of combined approaches using coolant improvement properties and a micro-fin tube.[9] Salehi *et al*.[10] examined the thermal efficiency of the closed thermosyphon under the magnetic field using ferrofluid as the working fluid. Ferrofluid's heat transfer in a pipe with a magnetic field was investigated by Ghofrani *et al*.[11] The temperature properties of the different coolants flowing in the channel were assessed using different corrugated profiles.[12]

[1] *Department of Agricultural Machinery Engineering, Faculty of Engineering and Architecture, Rajamangala University of Technology Isan, Nakhonratchasima, 30000, Thailand.*
[2] *Department of Pharmaceutical Chemistry, Faculty of Pharmacy, Srinakharinwirot University, 63 Rangsit-Nakhornnayok Rd., Ongkharak, Nakhorn-Nayok, 26120, Thailand.*
[3] *Department of Mechanical Engineering, Faculty of Engineering, Rajamangala University of Technology Isan, Khon Kaen Campus, 40000, Thailand.*

Yarahmadi *et al*.[13] studied the transport of laminar heat by forced convection under magnetic fields with various configurations and working modes. Many researchers have performed on the magnetohydrodynamic (MHD) heat transfer and flow characteristics in different thermal systems. This work has been continuously performed by Daniel *et al*.[14] This paper aims to consider the effect of buoyancy and thermal radiation on MHD flow over a stretching porous sheet. Based on the study result of Daniel *et al*.,[15-17] entropy analysis in electrical magnetohydrodynamic flow and double stratification effects on unsteady MHD of nanofluid have been considered, and slip role for unsteady MHD mixed convection of nanofluid over stretching sheet with thermal radiation and electric field has been investigated.[18] Sha *et al*.[19] investigated heat transfer characteristics of ferrofluids with the magnetic field effect. An average Nusselt number rose in oscillating and steady magnetic fields by 4.1 and 8.1 percent, respectively. Gui *et al*.[20] focused on using single-phase ferrofluids with an external magnetic field to enhance microchannel heat transmission. The analysis of the nanofluids heat transfer oscillation in the fluted tube was examined by Xin *et al*.[21] Shi *et al*.[22] studied the effects of the magnetic field on the thermophysical properties of Ferrosoferric oxide (Fe_3O_4) nanofluid and its capacity to regulate heat transfer efficiency. Naphon and Wiriyasart combined the active and passive methods for thermal cooling systems, considering corrugated tubes, magnetic fields, nanofluids, and pulsing flow.[23] Wang *et al*.[24] examined the grooved pitch concerning the efficiency of using magnetic fluid as a coolant. Mei *et al*.[25] have examined the magnetic direction effect on the thermal performance of various nanofluids in circular and corrugated tubes. And Wang *et al*.[26] The investigation focused on the thermal efficiency using nanofluid passing through various configurations of corrugated and circular tubes.[27-30] Next, Upalkar *et al*.[31] analyzed the corrugated tube's nanofluid's heat removal ability with a porous medium. Naphon *et al*.[32] used machine learning to study the flow resistance and heat removal ability of pulsing nanofluid flow in a corrugated tube with a magnetic field. Zhang *et al*. [33] considered the influences of tilt and magnetic field on natural heat transfer in a nanofluid cavity using a twofold Boltzmann technique. Using a magnetic fluid as the working fluid, Behzadnia *et al*.[34] improved the shape of the fluted tube. Next, the thermal cooling efficiency of single-phase and multiphase flow in the fluted tubes has been investigated.[35] The influence of nanofluid flow features, such as pulsing flow, nanofluid concentration, corrugated tube shapes, and heat flux, on the thermal efficiency with the magnetic field was recently examined by Siricharoenpanitch *et al*.[36,37]

As we have seen above, many works have been performed on the thermal efficiency of different working fluids in different thermal devices and application systems. Several studies have used magnetic fields and chemicals to enhance thermal performance. However, there has been little investigation into coupled heat transfer improvement schemes, notably the oscillation of an electromagnetic field. Due to the increasing surface heat transfer area, the disturbance boundary layer expands as the fluted tube develops. As a consequence, fluted tubes were discovered to be helpful in a variety of thermal systems. There has been limited investigation into how the electromagnetic field's rotating direction, power, and frequency affects the Brownian movement of particles floating in a based fluid. This work investigates the heat removal efficiency of ferrofluids in a fluted tube as a function of rotating frequency, power, rotating direction, and frequency of an electromagnetic field. For verification, the acquired data are compared to published results.

2. Experimental system and procedure

2.1 Experimental system and test section

The device is intended to investigate the thermal cooling effectiveness of ferrofluids in fluted tubes during an electromagnet field oscillation, as seen in Fig. S1. For coolant circulation in the closed coolant system, a reservoir tank containing ferrofluid is coupled to a variable magnetic pump. The weight-with-stop watch is used to measure the ferrofluid flow rate. Pneumatic connectors must be used for component connections because of the system's low pressure. The corrugated tube has inside diameter (D_i), outside diameters (D_o), and length (L) values of 1.02 cm, 1.27 cm, and 200 cm, respectively, as shown in Fig. S2. There are five thermocouples for coolant inside the test section tube and five outside surfaces, which are pre-calibrated using a standard calibrator. A pressure drop unit (YOKOKAWA) is applied to monitor the pressure drop. The thermocouples were protected from any changes in the magnetic field by magnetic shields. The test part is heated by a nickel-chromium heater wrapped around the test pipe, and an Aeroflex tube covers it as an insulator. The multimeter measures the power supply to the

[4] *Department of Mechanical Engineering, Faculty of Technology, Udon Thani Rajabhat University, Udon Thani, 41000, Thailand.*
[5] *Department of Mechanical Engineering, Faculty of Engineering, Mahanakorn University of Technology, Bangkok 10530, Thailand.*
[6] *Department of Mechanical Engineering, Faculty of Engineering, Srinakharinwirot University, 63 Rangsit-Nakhornnayok Rd., Ongkharak, Nakhorn-Nayok, 26120, Thailand.*
**Email:* paisarnn@g.swu.ac.th (P. Naphon)

electric wire heater. The fluted tube's axial direction of heat is reduced by adding polyurethane to both ends. The refrigeration cooling system keeps the inlet ferrofluids at a consistent temperature. The data taker (DT85 model) and computer unit, part of the data acquisition system, gather the pertinent parameters after the system has reached a steady state.

2.2 Electromagnet field system

The sixteen electromagnet units (four stations), monitor light bulb system, and Programmable Logic Controller (PLC) system comprise the electromagnetic field (EF) system. As shown in Fig. 1, the corrugated tube is placed between four electromagnet units, with four stations set up. The magnets are constructed from zinc ferrite powder cores wrapped in copper wire and insulated with iron powder and iron alloys. At each EF station, the electromagnetic unit operates independently. The power can change the electromagnetic flux of each electromagnet unit. The electromagnetic unit and the connecting/disconnecting times can be changed by the digital circuit control and controlled by the PLC system. By setting the connection/disconnection time to zero or alternative values, the EF conditions (frequency) may be generated. By altering the electromagnet unit's operating sequence, the rotating direction of the EF may be controlled. In addition, the frequency of rotation (each station) can be done by setting the overlap time of each electromagnetic unit.

Table 1. Thermo-physical properties of water, Fe_3O_4.[3]

Properties	Water	Fe_3O_4
Density, (kg/m^3)	996.88	5180
Thermal conductivity, (W/m.K)	0.6097	80.4
Viscosity, (mPa S)	0.728	-
Specific heat, (J/kg.K)	4181	670
Purity, %	-	>99.9
Average diameter, nm	-	23

2.3 Nanofluid preparation

Fe_3O_4 nanoparticles (Purity>99.9%) dissolved in the base fluid are stirred with some agent to obtain a pH of 8 using an ultrasonic system. The use of Fe_3O_4 nanoparticles with thermophysical properties (Table 1) in this work is based on the excellent response to the electromagnetic field. According to the sample's scanning electron microscope (SEM) image, most nanoparticles are roughly spherical, as illustrated in Fig. 2(a). Furthermore, the sonicated unit stimulated the nanofluid for 10 minutes every hour to obtain stability. The Spectrophotometer UV-1800 measures the % absorbance spectrum for the 1st and 2nd days of the fluids in Fig. 2(b). The % absorbance spectrum on the 1st and 2nd days was similar, with an error of 1.03%, which implies that it is still stable.

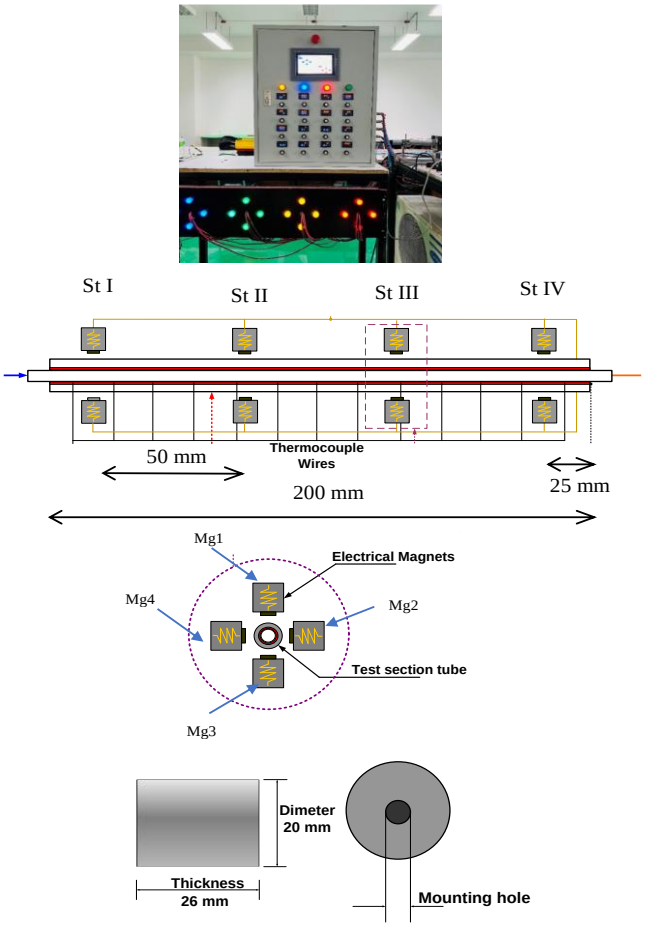

Fig. 1 Schematic diagram of the test section and located electromagnetic sources.

Table 2. Experimental conditions.

Parameters	Ranges
Power input (W)	400
Ferrofluid concentration (% by volume)	0.015
Ferrofluid Reynolds number	5000-10000
Rotation frequency of electromagnetic field (ms)	800-3200
Electromagnet field (μT)	0.5-30
Frequency of electromagnetic field (ms)	200-800

2.4 Experimental procedure

To reduce the impact on the environment, the test process was carried out with water/ferrofluids as the coolants flowed through the test section in the air conditioning room at 25 °C, and the inlet coolant temperature was maintained constant at 20 °C. Tests have been performed with different working flow rates, EF frequency, EF flux, and EF rotation direction and frequency. Table 2 provides a list of the test conditions of the present study. Given the relevant parameters, the flow rate is increased in small increments. As the system is steady, the results are recorded five times.

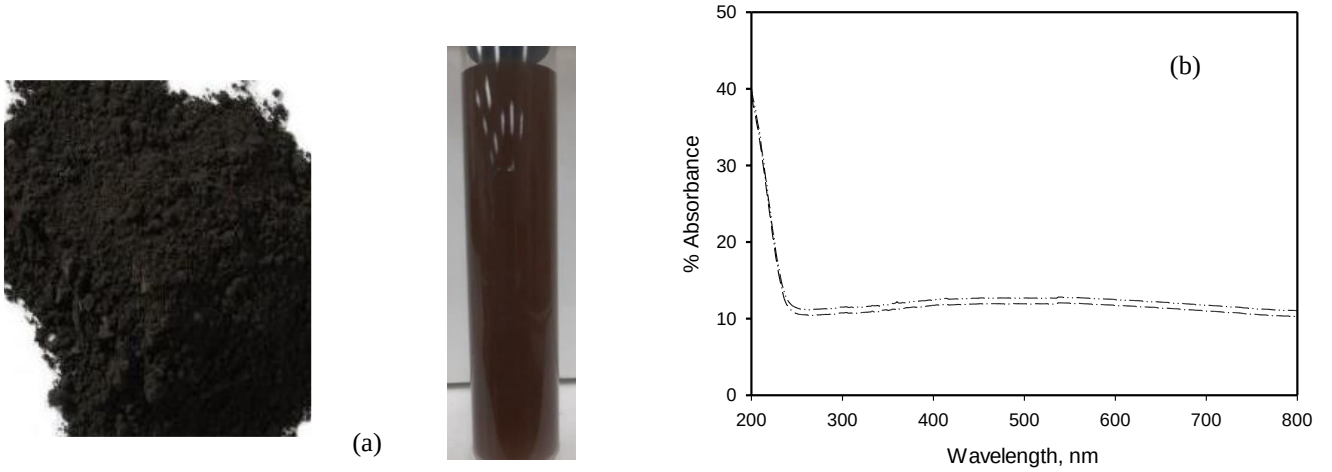

Fig. 2 Photograph of (a) the nanoparticles, ferrofluid, and (b) % absorbance by ferrofluid.

2.5 Electromagnetic frequency control procedure

A PLC control system has controlled the EF system's operating conditions. There are four electromagnetic stations (St. I, St. II, St. III, St. IV), and each station has four electromagnetic units, which operate independently. The digital circuit control can adjust the connecting and disconnecting time. The connecting/disconnecting time of zero is the result of the zero EF frequency, which electrical energy is fed to the electromagnet units at all times. Each electromagnetic unit's connecting/disconnecting time must be set to the same value to consider the frequency effect. This can be observed from the operation of the light bulbs of each electromagnetic unit, which will flash simultaneously. The electromagnetic frequency was calculated as the reciprocal of the pulse wave's period time, as seen in Fig. S3.

2.6 Electromagnetic field rotation direction procedure

Four electromagnetic stations (St. I, St. II, St. III, and St. IV) and each electromagnetic unit operate independently in the electromagnetic field system. Setting the overlap time of each electromagnetic unit can control the rotation frequency and rotating direction of the electromagnetic unit (at the same station). The rotation direction can be performed in clockwise and counterclockwise directions (Mg1, Mg2, Mg3, and Mg4) for clockwise direction, and Mg1, Mg4, Mg3, and Mg2 for counterclockwise direction). The light bulbs of each electromagnet unit will sequence the blinking depending on the rotation direction. The rotation directions of the electromagnetic field are found in Fig. 3.

2.7 Electromagnetic flux control procedure

EF strength can be changed by changing the power to each electromagnetic unit, which is monitored using the volts meter. The electromagnetic flux can be measured using the Gauss

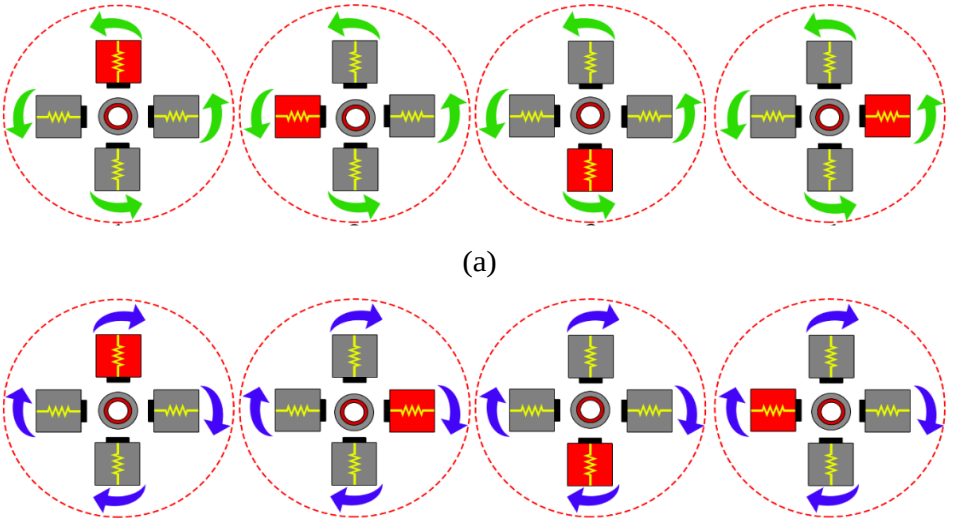

Fig. 3 shows the rotation direction of EF at the same station (a) counterclockwise direction (b) clockwise direction.

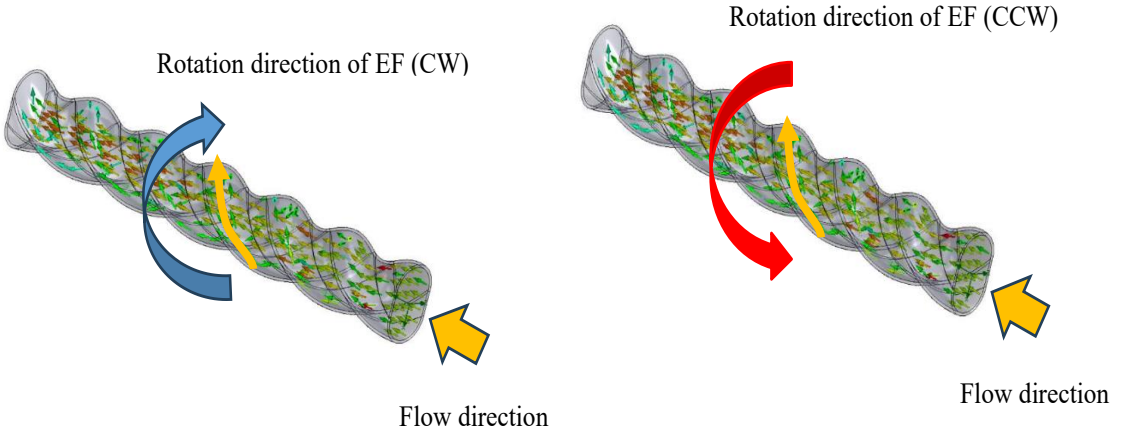

Fig. 4 shows the rotation direction of EF and the flow direction of the coolant.

meter (HT201 Gauss meter). The rotation directions of the electromagnetic field, as compared with the direction of the thread groove, can be seen in Fig. 4.

2.8. Data reduction and uncertainty analysis procedures

The Fe_3O_4/water nanofluid (Ferrofluid) heat transfer, supplied by the power, is measured, and the average heat transfer is calculated.

$$Q_{nf} = \dot{m}_{nf} C_{p_{nf}} (T_{in} - T_{out})_{nf} \quad (1)$$

$$Q_{heater} = IV \quad (2)$$

$$Q_{ave} = \frac{Q_{nf} + Q_{heater}}{2} \quad (3)$$

The characteristics of Fe_3O_4/water nanofluids are ascertained by using the suggested correlations as follows:[38,39]

$$\rho_{nf} = \varphi\rho_P + (1-\varphi)\rho_w \quad (4)$$

$$(\rho C_p)_{nf} = \phi(\rho C_p)_p + (1-\phi)(\rho C_p)_w \quad (5)$$

The formula may be applied to calculate the inside pipe surface:

$$T_{wi,ave} = T_{wo,ave} - \frac{Q_{ave} ln(r_o/r_i)}{2\pi k_w L} \quad (6)$$

The correlation for nanofluid thermal conductivity that has been presented is derived from:[40]

$$k_{nf} = \left[\frac{k_p + 2k_w - 2\varphi(k_w - k_p)}{k_p + 2k_w + \varphi(k_w - k_p)}\right] k_w \quad (7)$$

The following may be used to calculate the *Nu* and *h* :

$$h = \frac{Q_{ave}}{A(T_{wi,ave} - T_{nf,ave})} = \frac{[IV + (\rho A_{cr} U)_{nf} C_{pnf} (T_{in,nf} - T_{out,nf})]/2}{\pi DL(T_{wi,ave} - T_{nf,ave})} \quad (8)$$

$$Nu = \frac{hD}{k_{nf}} \quad (9)$$

The following factors influence the viscosity of nanofluid:[41]

$$\mu_{nf} = (1 + 2.5\varphi)\mu_w \quad (10)$$

The following is the basis for calculating the friction factor (*f*):

$$f = \frac{\Delta P}{\left(\frac{\rho_{nf} U_{nf}^2}{2}\right)\left(\frac{L}{D}\right)} \quad (11)$$

Table 3. Uncertainty and accuracy of the instruments.

Instruments	Accuracy	Uncertainty
Voltage supplied by power source, voltage	0.2%	±0.5
Current supplied by power source, ampere	0.2%	±0.5
Digital weight scale, gram	0.01%	±0.01
Thermocouple type T, Data logger, °C	0.1%	±0.1
Differential pressure transducer	0.02%	±0.02

The uncertainty of measurement findings is computed using the Coleman and Steel technique.[42] The Nusselt number (*Nu*) in this investigation depends on tube wall temperatures, coolant temperatures, and coolant velocity. The coolant velocity and the pressure drop influence the flow resistance. This data may be used to calculate the uncertainty of the *f* and *Nu*.

$$\frac{\partial Nu}{Nu} = \sqrt{\left(\frac{\partial Nu}{U}\right)^2 + \left(\frac{\partial Nu}{T_{wi,ave}}\right)^2 + \left(\frac{\partial Nu}{T_{wo,ave}}\right)^2 + \left(\frac{\partial Nu}{T_{nf,ave}}\right)^2 + \left(\frac{\partial Nu}{T_{in,nf}}\right)^2 + \left(\frac{\partial Nu}{T_{out,nf}}\right)^2} \quad (12)$$

$$\frac{\partial f}{f} = \sqrt{\left(\frac{\partial f}{U}\right)^2 + \left(\frac{\partial f}{(\Delta P)}\right)^2} \quad (13)$$

Calculating uncertainty also requires the qualities of the essential parameters, the operating circumstances, and the accuracy and uncertainty of the relevant measured devices, as indicated in Table 3. *Nu* and *f* have maximum uncertainties of ±5.2 % and ±7.3 %, respectively. (Steel and Coleman,[37]).

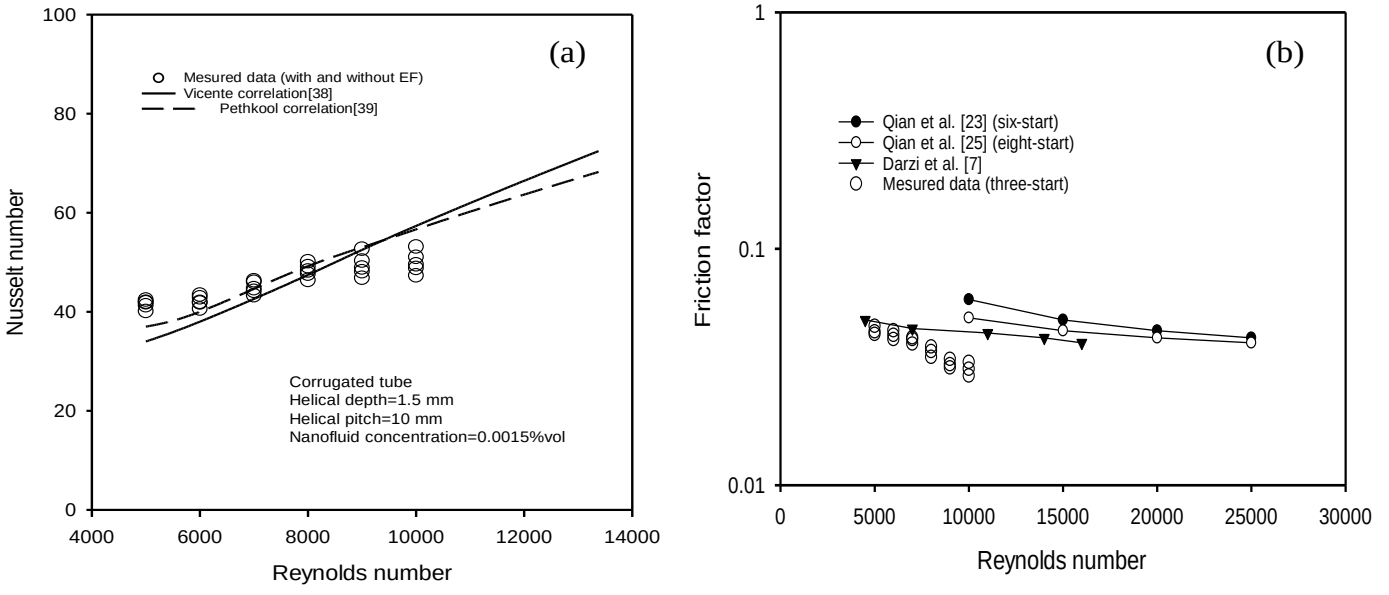

Fig. 5 Comparison of the measured results with the proposed correlations for (a) Nusselt number and (b) friction factor.

3. Results and discussion

3.1 Setup system verification

In the current work, the coolant enters the test tube under circumstances of steady heat flux. Verifying the results with helical ribs is done using the correlations.[43,44] The correlation of Vicente *et al*.[43] and Pethkool *et al*.[44] is also compared with the measured Nu in the following manner:

$$Nu = 0.403\left(\frac{e}{D_i}\right)^{0.53}\left(\frac{p}{D_i}\right)^{-0.29}(Re-1500)^{0.74}Pr^{0.64} \quad (14)$$

$$Nu = 1.579\,Re^{0.639}\left(\frac{e}{D_i}\right)^{0.30}\left(\frac{p}{D_i}\right)^{0.35} \quad (15)$$

A validation experiment is performed to determine whether the experimental system is reliable. Fig. 5a illustrates that the error of the Nusselt number is within 3.53 %, indicating that the testing system may be considered reliable based on comparing the experimental findings with other data obtained by published Refs. [43, 44]. Furthermore, Fig. 5b compares the expected data from the measured data and the calculated friction factor from the current investigation. The statistics from Ref. [7, 28, 30] have indicated an accuracy of 11.25 %, 8.4 %, and 4.53 %, respectively. The shape and angle of the corrugation, which are crucial for determining the flow resistance and heat removal ability along these tubes, may be formed by the fluted tube's construction process. As seen in Fig. 5b, one of the possible reasons for disagreement might be associated with the corrugation angles and the fabrication process.

3.2 Effect of electromagnetic flux

The impact of electromagnetic fluxes on the *Nu* is seen in Fig. 6. Reduced boundary layer thickness and increased effective thermal conductivity are proposed as the two main elements boosting the convective heat transfer of nanofluids. First, the Brownian nanoparticle movement disrupted the boundary zone, increasing convective heat transmission. Second, the turbulent intensity transported particles across the turbulent flow regime, improving mixing and aiding in the transmission of thermal energy. The heat removal ability was marginally enhanced. Therefore, the *Nu* for the nanofluid is more than that for deionized water, as shown in Fig. 6. The Fe_3O_4 nanoparticles utilized in this study have a higher magnetic field sensitivity. Four electromagnet units have been installed and are operating normally with the main flow of coolant.

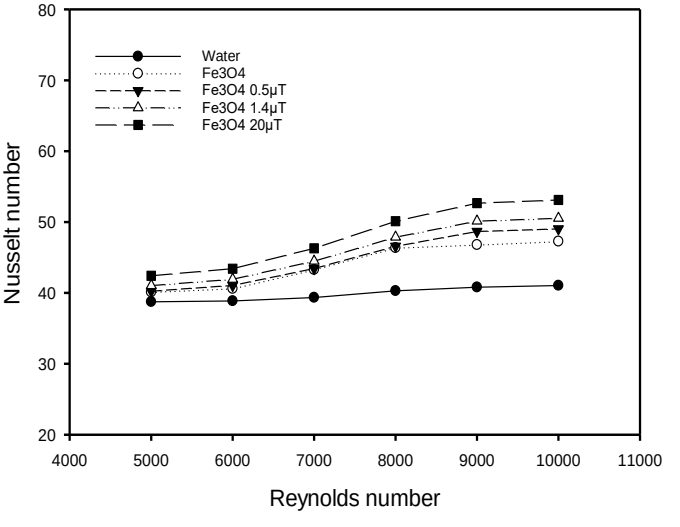

Fig. 6 Variation of Nusselt number with Reynolds number for different EF fluxes.

Each magnetic unit's connecting/disconnecting time establishes the same value (Zero values). The zero electromagnetic frequency, which supplies electrical energy to the electromagnet units continuously, causes the connecting/disconnecting time to be zero. The electromagnetic field causes the nanoparticles to migrate toward the tube wall, substantially affecting the boundary zone disturbance.

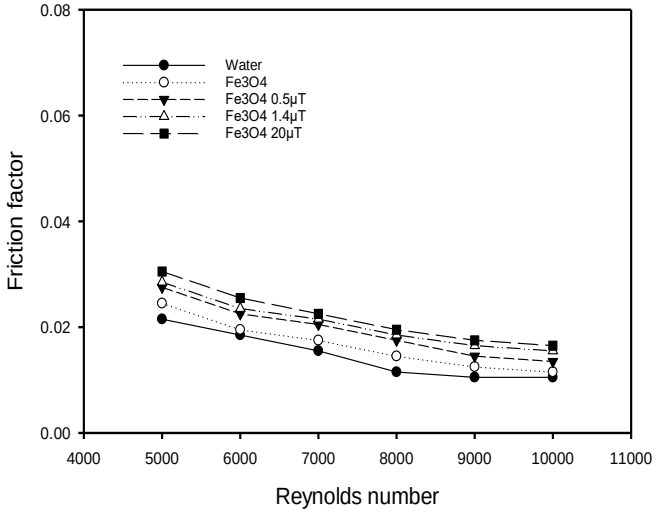

Fig. 7 Variation of friction factor with Reynolds number for different EF fluxes.

Moreover, more electromagnetic flux strength increases nanoparticles' turbulence intensity and local thermal conductivity. Consequently, for three distinct electromagnetic fluxes, the Nusselt number improves by 2.54 %, 5.32 %, and 12.32 %. Additionally, the *Nu* for ferrofluid as a coolant is more significant than that of water because of the increased turbulence intensity and higher mixing of nanoparticles. As previously shown, the particles go toward the pipe wall, overcoming the increased roughness and the main flow. According to Fig. 7, the flow *f* with an EF is 5.76 %, 9.34 %, and 15.04 % more than those without an electromagnetic field.

3.3 Effect of electromagnetic frequency

Figure 8 illustrates how the Reynolds and Nusselt numbers change at various electromagnetic frequencies. Multiple values of the connecting/disconnecting time lead to varying EF frequencies, in which each magnetic unit's connecting/disconnecting time establishes the same value. How each electromagnet unit operates-its light bulbs will flash simultaneously-allows one to see this. As shown in Fig. S3, the electromagnetic field frequency was determined as the reciprocal of the period time of the pulse wave. It is thought that transverse movement of magnetic nanoparticles (connection time) and movement along the tube (disconnecting time) induce nanoparticle migration, thermal boundary layer disturbances, and turbulent intensity, all of which are related to electromagnetic frequency. The Nu rises when particles move and are attracted to the pipe wall in a short period of time (high frequency), reducing the thickness of the thermal barrier zone. Therefore, a higher *Nu* results from increased electromagnetic frequency, as shown in Fig. 8. At the same electromagnetic flux of 20 μT, the Nusselt number at an electromagnetic frequency of 200 ms is 8.97 % more than 0 ms. As previously demonstrated, the particles overcome the core flow and the tube wall's enhanced roughness by moving toward the wall. The *f* under oscillation EF is 2.37 %, 3.57 %, and 5.98 % higher than those stationary, as shown in Fig. 9.

3.4 Effect of electromagnetic rotation direction

Four electromagnetic units and four electromagnet stations (St. I, St. II, St. III, and St. IV) function independently in the electromagnetic field system. By adjusting each electromagnetic unit's overlap duration, the electromagnetic

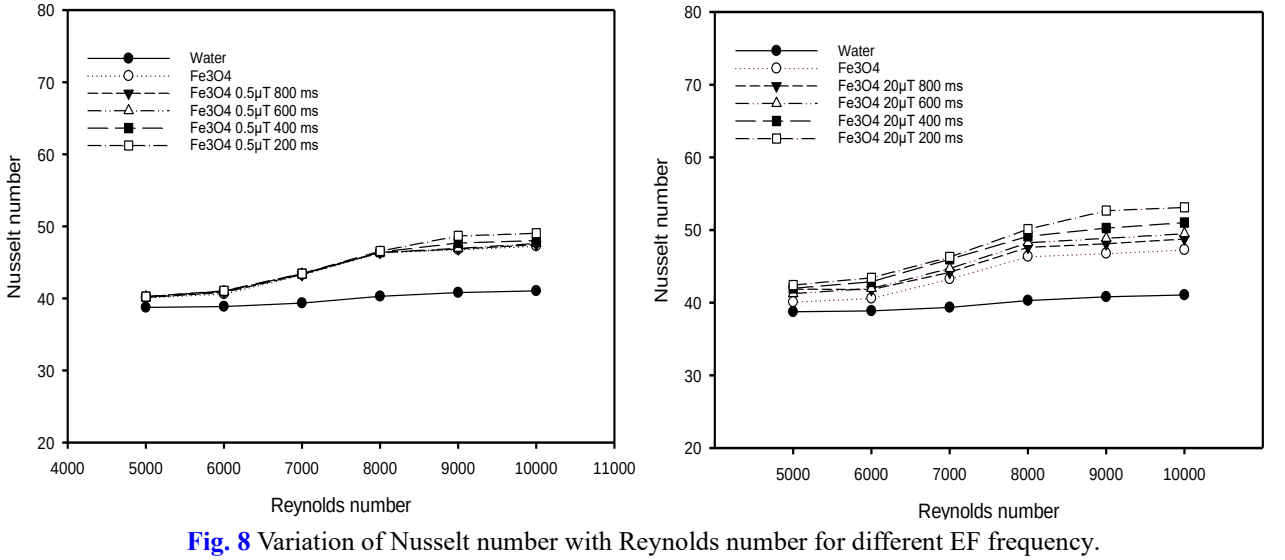

Fig. 8 Variation of Nusselt number with Reynolds number for different EF frequency.

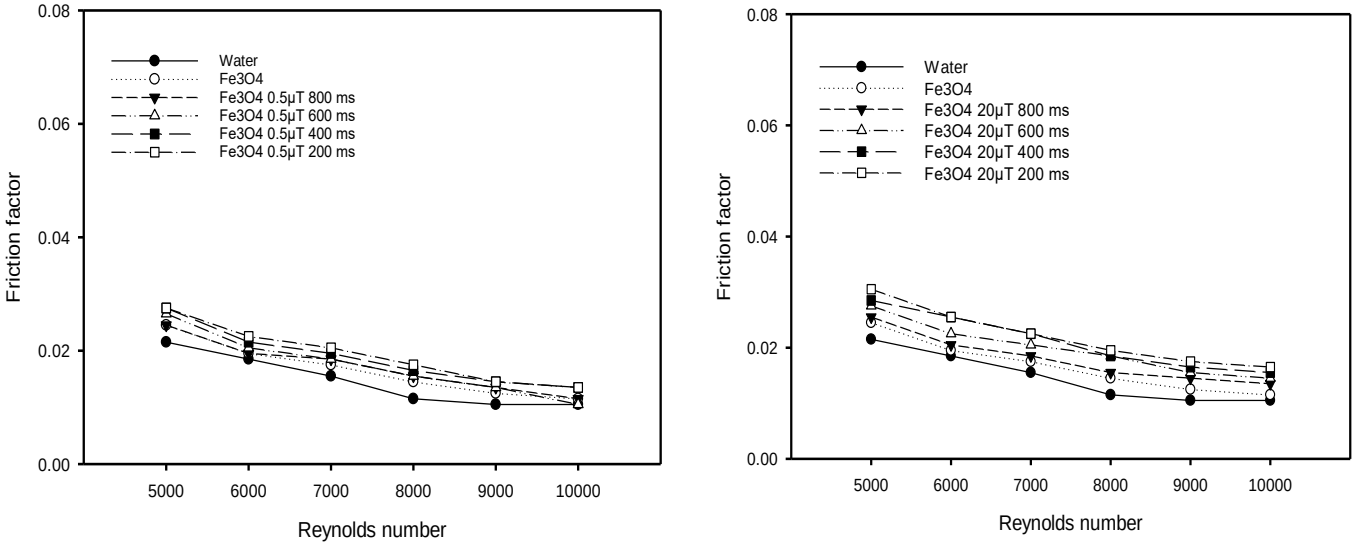

Fig. 9 Variation of friction factor with Reynolds number for different EF frequency.

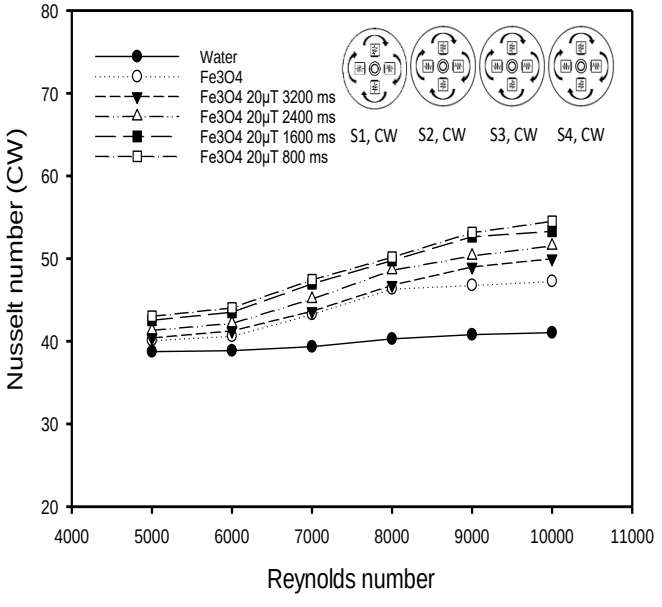

Fig. 10 Variation of Nusselt number with Reynolds number for clockwise rotation EF.

unit's rotation frequency (at the same station) may be set. The direction of rotation can be executed in two ways: clockwise (Mg1, Mg2, Mg3, and Mg4) and counterclockwise (Mg1, Mg4, Mg3, and Mg2), as seen in Fig. 3, in which monitored from the light bulbs of each electromagnet unit will sequence the blinking depending on the rotation direction. Figs. 10 and 11 show the variations of the *Nu* and *f* with the *Re* for different EF rotation frequencies (clockwise direction). The tube surface influences the direction and severity of turbulence, especially near the tube wall. The increase in turbulence strength reveals mixing from the main region to the wall and indicates the degree of variance. As one moves away from the boundary layer, the fluid oscillation level declines from its peak near the tube wall. The flow along the wall follows the corrugated groove in a circular pattern. As seen in Fig. 4a, the primary flow is still parallel to the tube. Because of the electromagnetic field, the particles migrate to the wall, and the rotation moves along the direction of the corrugated groove and the direction of the electromagnetic field rotation. As a result, the velocity near the wall rises compared to when the EF rotation is absent, in which the turbulent intensity significantly affects the rising heat transfer. As a result, the *Nu* increases in value with increasing EF rotation frequency and is more significant with EF rotation than without it. The *f* with an EF rotation frequency is 2.45 %, 3.76 %, and 6.21 % higher than those without an EF rotation, as shown in Fig. 11.

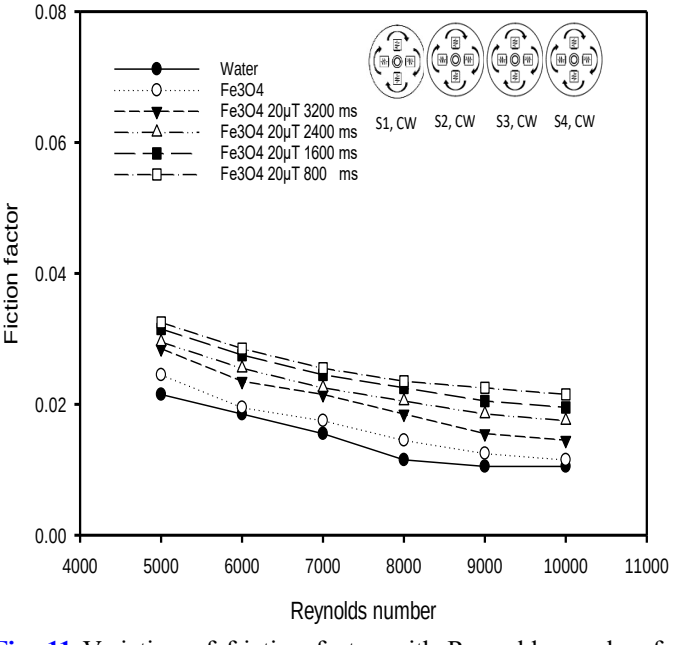

Fig. 11 Variation of friction factor with Reynolds number for clockwise rotation EF.

The primary flow remains parallel to the tube in the counterclockwise direction, while the flow close to the wall follows the corrugated groove in a circular direction. As shown in Fig. 4b, the rotation goes against the direction of the fluted groove, causing the particles to migrate to the wall due to the electromagnetic field. This causes greater turbulence intensity and thermal zone disturbances. Figs. 12 and 13 show that the *Nu* and *f* for EF in a counterclockwise rotating direction are more prominent than in stationary. It is more important with EF rotation than without, and its value increases with EF rotation frequency. As previously stated, the mobility of nanoparticles is strongly controlled by clockwise and counterclockwise electromagnetic rotation orientations.

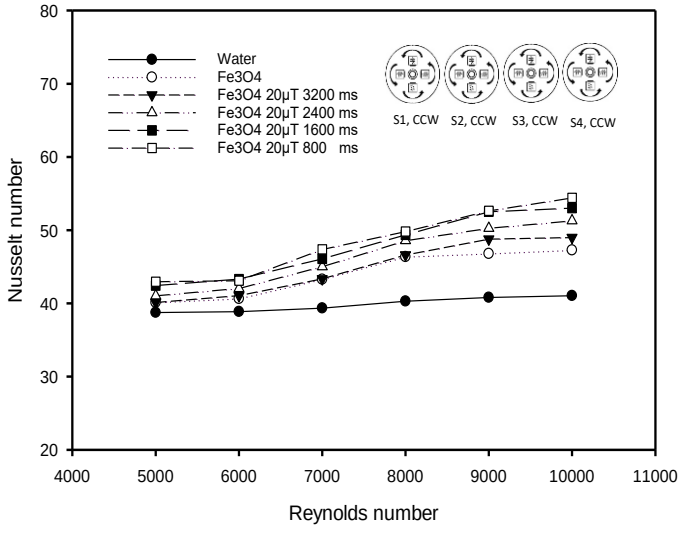

Fig. 12 Variation of Nusselt number with Reynolds number for counterclockwise rotation EF.

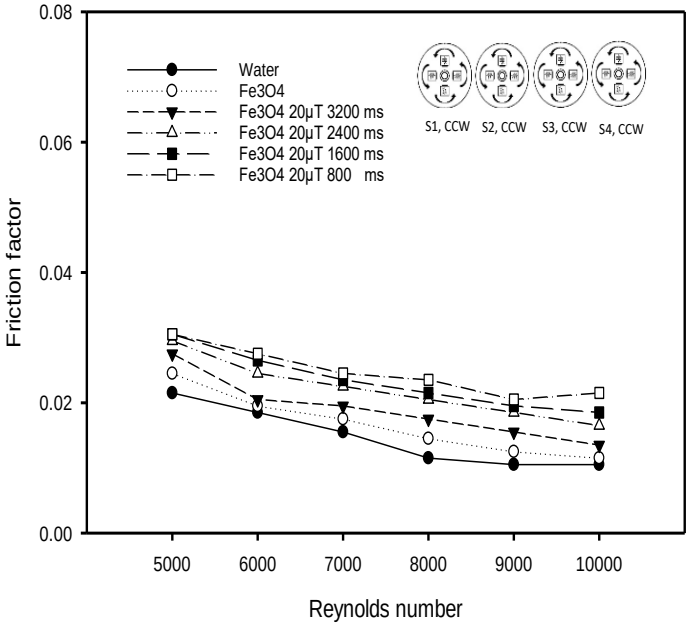

Fig. 13 Variation of friction factor with Reynolds number for counterclockwise rotation EF.

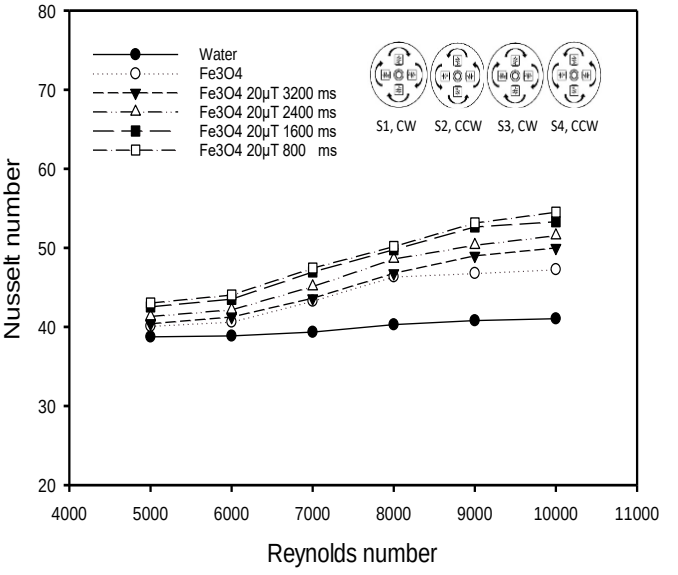

Fig. 14 Variation of Nusselt number with Reynolds number for alternating rotation EF.

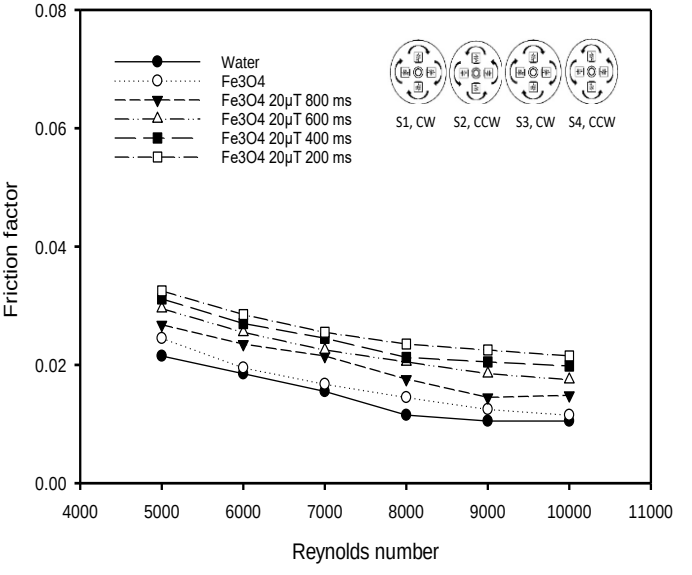

Fig. 15 Variation of friction factor with Reynolds number for alternating rotation EF.

This results in increased fluid velocity along the tube wall, greater mixing levels, thermal zone disruption, and turbulent intensity. Figs. 14 and 15 show the effects of switching EF rotation direction on *Nu* and *f* at different EF rotation frequencies. Both data reveal that the most significant increases in Nu and f are 15.54% and 15.87%, respectively, when compared to the absence of an electromagnetic field.

4. Conclusion

This work used a constant and oscillating electromagnetic field to experimentally study ferrofluid's heat removal ability and flow resistance moving through a fluted tube. The migration, turbulence intensity, and thermal zone disturbances

caused by the transverse migration of nanoparticles (connection time) and the movement along the tube (disconnecting time) are all related to the electromagnetic frequency. Furthermore, the clockwise and counterclockwise electromagnetic rotation directions substantially affect the rotation of nanoparticle movement. As a result, there is an increase in turbulence intensity, mixing level, thermal boundary layer disturbance, and fluid velocity close to the tube wall. When an oscillating electromagnet field is applied to a fluted tube, the Nusselt number of ferrofluids produced is more than when a station electromagnet field is applied and higher than when EF is not present. However, the impact of certain other important characteristics should be investigated further. The findings of this research are utilized to provide a knowledge base that can be used to design and manufacture heat transfer devices that improve thermal performance while decreasing system energy consumption.

Nomenclature

A surface area, (m^2)
C_p specific heat, ($kJkg^{-1}\ ^oC^{-1}$)
D diameter, (m)
EF electromagnetic field
f friction factor, (-)
h heat transfer coefficient, ($kWm^{-2}\ ^oC^{-1}$)
k thermal conductivity, ($kWm^{-1}\ ^oC^{-1}$)
I electrical current, (A)
L tube length, (m)
$\dot{m}$ mass flow rate, (kgs^{-1})
Nu Nusselt number, (-)
P pressure, (kNm^{-2})
Pr Prandtl number, (-)
Q heat transfer rate, (kW)
Re Reynolds number, (-)
T temperature, (^oC)
U velocity, (ms^{-1})
V voltage, (V)

Greek symbol

φ nanofluids concentration, (%vol.)
ρ density, (kgm^{-3})
μ viscosity, ($kg\ m^{-1}s^{-1}$)

Subscripts

ave average
heater heater
in inlet
i inner
nf nanofluids
p particles
o outer
out outlet
w water

Acknowledgments

The authors would like to thank Srinakharinwirot University's (SWU) Faculty of Engineering for the financial assistance with this study.

Conflict of Interest

There is no conflict of interest.

Supporting Information

Applicable.

References

[1] Q. Li, Y. Xuan, J. Wang, Experimental investigations on transport properties of magnetic fluids, *Experimental Thermal and Fluid Science*, 2005, **30**, 109-116, doi: 10.1016/j.expthermflusci.2005.03.021.
[2] Q. Li, Y. Xuan, Experimental investigation on heat transfer characteristics of magnetic fluid flow around a fine wire under the influence of an external magnetic field, *Experimental Thermal and Fluid Science*, 2009, **33**, 591-596, doi: 10.1016/j.expthermflusci.2008.12.003.
[3] M. Lajvardi, J. Moghimi-Rad, I. Hadi, A. Gavili, T. Dallali Isfahani, F. Zabihi, J. Sabbaghzadeh, Experimental investigation for enhanced ferrofluid heat transfer under magnetic field effect, *Journal of Magnetism and Magnetic Materials*, 2010, **322**, 3508-3513, doi: 10.1016/j.jmmm.2010.06.054.
[4] Y. Iwamoto, H. Yamaguchi, X.-D. Niu, Magnetically-driven heat transport device using a binary temperature-sensitive magnetic fluid, *Journal of Magnetism and Magnetic Materials*, 2011, **323**, 1378-1383, doi: 10.1016/j.jmmm.2010.11.050.
[5] A. A. R. Darzi, M. Farhadi, K. Sedighi, R. Shafaghat, K. Zabihi, Experimental investigation of turbulent heat transfer and flow characteristics of SiO_2/water nanofluid within helically corrugated tubes, *International Communications in Heat and Mass Transfer*, 2012, **39**, 1425-1434, doi: 10.1016/j.icheatmasstransfer.2012.07.027.
[6] A. A. R. Darzi, M. Farhadi, K. Sedighi, S. Aallahyari, M. A. Delavar, Turbulent heat transfer of Al_2O_3–water nanofluid inside helically corrugated tubes: numerical study, *International Communications in Heat and Mass Transfer*, 2013, **41**, 68-75, doi: 10.1016/j.icheatmasstransfer.2012.11.006.
[7] A. Ali Rabienataj Darzi, M. Farhadi, K. Sedighi, Experimental investigation of convective heat transfer and friction factor of

Al2o3/water nanofluid in helically corrugated tube, *Experimental Thermal and Fluid Science*, 2014, **57**, 188-199, doi: 10.1016/j.expthermflusci.2014.04.024.
[8] C. Qi, Y.-L. Wan, C.-Y. Li, D.-T. Han, Z.-H. Rao, Experimental and numerical research on the flow and heat transfer characteristics of TiO_2-water nanofluids in a corrugated tube, *International Journal of Heat and Mass Transfer*, 2017, **115**, 1072-1084, doi: 10.1016/j.ijheatmasstransfer.2017.08.098.
[9] K. Wongcharee, S. Eiamsa-ard, Heat transfer enhancement by using CuO/water nanofluid in corrugated tube equipped with twisted tape, *International Communications in Heat and Mass Transfer*, 2012, **39**, 251-257, doi: 10.1016/j.icheatmasstransfer.2011.11.010.
[10] H. Salehi, S. Zeinali Heris, F. Sharifi, M. A. Razbani, Effects of a nanofluid and magnetic field on the thermal efficiency of a two-phase closed thermosyphon, *Heat Transfer—Asian Research*, 2013, **42**, 630-650, doi: 10.1002/htj.21043.
[11] A. Ghofrani, M. H. Dibaei, A. Hakim Sima, M. B. Shafii, Experimental investigation on laminar forced convection heat transfer of ferrofluids under an alternating magnetic field, *Experimental Thermal and Fluid Science*, 2013, **49**, 193-200, doi: 10.1016/j.expthermflusci.2013.04.018.
[12] M. A. Ahmed, M. Z. Yusoff, K. C. Ng, N. H. Shuaib, Effect of corrugation profile on the thermal–hydraulic performance of corrugated channels using CuO-water nanofluid, *Case Studies in Thermal Engineering*, 2014, **4**, 65-75, doi: 10.1016/j.csite.2014.07.001.
[13] M. Yarahmadi, H. Moazami Goudarzi, M. B. Shafii, Experimental investigation into laminar forced convective heat transfer of ferrofluids under constant and oscillating magnetic field with different magnetic field arrangements and oscillation modes, *Experimental Thermal and Fluid Science*, 2015, **68**, 601-611, doi: 10.1016/j.expthermflusci.2015.07.002.
[14] Y. S. Daniel, S. K. Daniel, Effects of buoyancy and thermal radiation on MHD flow over a stretching porous sheet using homotopy analysis method, *Alexandria Engineering Journal*, 2015, **54**, 705-712, doi: 10.1016/j.aej.2015.03.029.
[15] Y. S. Daniel, Z. A. Aziz, Z. Ismail, F. Salah, Entropy analysis in electrical magnetohydrodynamic (MHD) flow of nanofluid with effects of thermal radiation, viscous dissipation, and chemical reaction, *Theoretical and Applied Mechanics Letters*, 2017, **7**, 235-242, doi: 10.1016/j.taml.2017.06.003.
[16] Y. S. Daniel, Z. A. Aziz, Z. Ismail, F. Salah, Double stratification effects on unsteady electrical MHD mixed convection flow of nanofluid with viscous dissipation and Joule heating, *Journal of Applied Research and Technology*, 2017, **15**, 464-476, doi: 10.1016/j.jart.2017.05.007.
[17] Y. S. Daniel, Z. A. Aziz, Z. Ismail, A. Bahar, F. Salah, Stratified electromagnetohydrodynamic flow of nanofluid supporting convective role, *Korean Journal of Chemical Engineering*, 2019, **36**, 1021-1032, doi: 10.1007/s11814-019-0247-5.
[18] Y. S. Daniel, Z. A. Aziz, Z. Ismail, A. Bahar, F. Salah, Slip role for unsteady MHD mixed convection of nanofluid over stretching sheet with thermal radiation and electric field, *Indian Journal of Physics*, 2020, **94**, 195-207, doi: 10.1007/s12648-019-01474-y.
[19] L. Sha, Y. Ju, H. Zhang, The influence of the magnetic field on the convective heat transfer characteristics of Fe_3O_4/water nanofluids, *Applied Thermal Engineering*, 2017, **126**, 108-116, doi: 10.1016/j.applthermaleng.2017.07.150.
[20] N. Gan Jia Gui, C. Stanley, N.-T. Nguyen, G. Rosengarten, Ferrofluids for heat transfer enhancement under an external magnetic field, *International Journal of Heat and Mass Transfer*, 2018, **123**, 110-121, doi: 10.1016/j.ijheatmasstransfer.2018.02.100.
[21] F. Xin, Z. Liu, N. Zheng, P. Liu, W. Liu, Numerical study on flow characteristics and heat transfer enhancement of oscillatory flow in a spirally corrugated tube, *International Journal of Heat and Mass Transfer*, 2018, **127**, 402-413, doi: 10.1016/j.ijheatmasstransfer.2018.06.139.
[22] L. Shi, Y. He, Y. Hu, X. Wang, Thermophysical properties of Fe_3O_4@CNT nanofluid and controllable heat transfer performance under magnetic field, *Energy Conversion and Management*, 2018, **177**, 249-257, doi: 10.1016/j.enconman.2018.09.046.
[23] P. Naphon, S. Wiriyasart, Pulsating flow and magnetic field effects on the convective heat transfer of TiO_2-water nanofluids in helically corrugated tube, *International Journal of Heat and Mass Transfer*, 2018, **125**, 1054-1060, doi: 10.1016/j.ijheatmasstransfer.2018.05.015.
[24] G. Wang, C. Qi, M. Liu, C. Li, Y. Yan, L. Liang, Effect of corrugation pitch on thermo-hydraulic performance of nanofluids in corrugated tubes of heat exchanger system based on exergy efficiency, *Energy Conversion and Management*, 2019, **186**, 51-65, doi: 10.1016/j.enconman.2019.02.046.
[25] S. Mei, C. Qi, T. Luo, X. Zhai, Y. Yan, Effects of magnetic field on thermo-hydraulic performance of Fe_3O_4-water nanofluids in a corrugated tube, *International Journal of Heat and Mass Transfer*, 2019, **128**, 24-45, doi: 10.1016/j.ijheatmasstransfer.2018.08.071.
[26] J. Wang, G. Li, H. Zhu, J. Luo, B. Sundén, Experimental investigation on convective heat transfer of ferrofluids inside a pipe under various magnet orientations, *International Journal of Heat and Mass Transfer*, 2019, **132**, 407-419, doi: 10.1016/j.ijheatmasstransfer.2018.12.023.
[27] Y. Zhang, F. Zhou, J. Kang, Flow and heat transfer in drag-reducing polymer solution flow through the corrugated tube and circular tube, *Applied Thermal Engineering*, 2020, **174**, 115185, doi: 10.1016/j.applthermaleng.2020.115185.
[28] J.-Y. Qian, C. Yang, Z. Wu, X.-L. Liu, X.-F. Gao, Z.-J. Jin, B. Sunden, Analysis of fouling in six-start spirally corrugated tubes, *Heat Transfer Engineering*, 2020, **41**, 1885-1900, doi: 10.1080/01457632.2019.1675246.
[29] C. Yang, G. Liu, J. Zhang, J.-Y. Qian, Thermohydraulic analysis of hybrid smooth and spirally corrugated tubes, *International Journal of Thermal Sciences*, 2020, **158**, 106520, doi: 10.1016/j.ijthermalsci.2020.106520.
[30] J.-Y. Qian, C. Yang, M.-R. Chen, Z.-J. Jin, Thermohydraulic performance evaluation of multi-start spirally corrugated tubes,

International Journal of Heat and Mass Transfer, 2020, **156**, 119876, doi: 10.1016/j.ijheatmasstransfer.2020.119876.
[31] S. A. Upalkar, S. Kumar, S. Krishnan, Analysis of fluid flow and heat transfer in corrugated porous fin heat sinks, *Heat Transfer Engineering*, 2021, **42**, 1539-1556, doi: 10.1080/01457632.2020.1807099.
[32] P. Naphon, T. Arisariyawong, S. Wiriyasart, A. Srichat, ANFIS for analysis friction factor and Nusselt number of pulsating nanofluids flow in the fluted tube under magnetic field, *Case Studies in Thermal Engineering*, 2020, **18**, 100605, doi: 10.1016/j.csite.2020.100605.
[33] T. Zhang, D. Che, Y. Zhu, H. Shi, D. Chen, Effects of magnetic field and inclination on natural convection in a cavity filled with nanofluids by a double multiple-relaxation-time thermal lattice boltzmann method, *Heat Transfer Engineering*, 2020, **41**, 252-270, doi: 10.1080/01457632.2018.1528057.
[34] H. Behzadnia, H. Jin, M. Najafian, M. Hatami, Geometry optimization for a rectangular corrugated tube in supercritical water reactors (SCWRs) using alumina-water nanofluid as coolant, *Energy*, 2021, **221**, 119850, doi: 10.1016/j.energy.2021.119850.
[35] C. Yang, M.-R. Chen, J.-Y. Qian, Z. Wu, Z.-J. Jin, B. Sunden, Heat transfer study of a hybrid smooth and spirally corrugated tube, *Heat Transfer Engineering*, 2021, **42**, 242-250, doi: 10.1080/01457632.2019.1699292.
[36] A. Siricharoenpanitch, S. Wiriyasart, P. Vengsungnle, N. Naphon, P. Naphon, Heat transfer of ferrofluid in fluted tubes with an electromagnetic field, *Heat Transfer Engineering*, 2023, **44**, 426-441, doi: 10.1080/01457632.2022.2068219.
[37] A. Siricharoenpanitch, S. Wiriyasart, P. Vengsungnle, N. Naphon, P. Naphon, Heat transfer and flow behaviors of ferrofluid in three-start helically fluted tubes, *Heat Transfer Engineering*, 2022, **43**, 1769-1782, doi: 10.1080/01457632.2021.2009227.
[38] B. C. Pak, Y. I. Cho, Hydrodynamic and heat transfer study of dispersed fluids with submicron metallic oxide particles, *Experimental Heat Transfer*, 1998, **11**, 151-170, doi: 10.1080/08916159808946559.
[39] Y. Xuan, W. Roetzel, Conceptions for heat transfer correlation of nanofluids, *International Journal of Heat and Mass Transfer*, 2000, **43**, 3701-3707, doi: 10.1016/s0017-9310(99)00369-5.
[40] D. Drew, S. Passman, Theory of multicomponent fluids, 1998.
[41] J. C. Maxwell, A Treatise on Electricity and Magnetism, 2010.
[42] H. W. Coleman, Experimental and Uncertainty Analysis for Engineers, 1989.
[43] P. G. Vicente, A. García, A. Viedma, Experimental investigation on heat transfer and frictional characteristics of spirally corrugated tubes in turbulent flow at different Prandtl numbers, *International Journal of Heat and Mass Transfer*, 2004, **47**, 671-681, doi: 10.1016/j.ijheatmasstransfer.2003.08.005.
[44] S. Pethkool, S. Eiamsa-ard, S. Kwankaomeng, P. Promvonge, Turbulent heat transfer enhancement in a heat exchanger using helically corrugated tube, *International Communications in Heat and Mass Transfer*, 2011, **38**, 340-347, doi: 10.1016/j.icheatmasstransfer.2010.11.014.

